An Improved Underdamped Asymmetric Bistable Stochastic Resonance Method and Its Application for Spindle Bearing Fault Diagnosis

PING XIA[1,2], **HUA XU**[1,2], **MOHAN LEI**[1], **AND SHENGLUN ZHANG**[1,2]

[1]School of Mechanical Engineering, Xi'an Jiaotong University, Xi'an 710049, China
[2]State Key Laboratory of Education Ministry for Modern Design and Rotor-Bearing System, Xi'an Jiaotong University, Xi'an 710049, China

Corresponding author: Ping Xia (qpingxia@hotmail.com)

ABSTRACT High-precision spindle bearing is one of the most critical and vulnerable parts in a motorized spindle. Its unexpected failure may lead to production loss. Stochastic resonance (SR) is a weak signal detection method, which can obtain noise energy in strong background noise and enhance incipient fault characteristics of spindle bearing. Based on the fact that asymmetry can improve the enhancement ability of asymmetric bistable SR in weak feature extraction, we introduce an underdamped well-width asymmetric bistable SR (UABSR) method to the field of bearing fault diagnosis for the first time. However, the engineering application of UABSR can still be limited by two aspects. Firstly, the SNR index can take effect only when the actual fault frequency is obtained in advance, so the UABSR method is at high-cost in real practices. Secondly, an appropriate band-pass filter band range of the bearing faults can hardly be obtained due to the massive impulsive noise in operations. Here an improved UABSR method for spindle bearing fault diagnosis is proposed. Infogram method is used to process and analysis the original vibration signal for resisting the influence from the impulsive noise and obtaining more accurate frequency range of spindle bearing fault. In addition, time domain zero-crossing (TDZC) index, as the index of the improved UABSR method, can directly reflect the fault characteristics of spindle bearings without knowing the accurate fault characteristic frequency in advance. Besides, the Quantum Genetic Algorithms (QGAs) and the fourth-order Runge-Kutta algorithm are combined to simultaneously obtain the optimal system parameter, the asymmetric ratio, the damping factor and the rescaling factor of the improved UABSR model. Comparing the Infogram and original UABSR methods, the improved UABSR method performs better effect in incipient spindle bearing fault diagnosis.

INDEX TERMS Spindle rolling bearing, fault diagnosis, underdamped asymmetric bistable stochastic resonance, vibration signal analysis, time domain zero-crossing index.

I. INTRODUCTION

High-precision angular contact hybrid ceramic ball bearing is a typical rolling bearing, which is widely used in many rotating machinery, especially the electric spindles, because its dynamic contact capacity of each rolling body relative to the raceway can bear the radial and axial forces [1]. Therefore, the design and manufacturing level, assembly and service performance of the spindle bearings directly determine the machining capability of machine tool spindles. And the spindle bearing is one of the most critical and vulnerable

The associate editor coordinating the review of this manuscript and approving it for publication was Yanzheng Zhu.

components in motorized spindle, whose unexpected failure will lead to production loss [2], [3]. Impulsive noise is inevitable in the actual engineering environment. In addition, the fault location of the spindle bearing and the range of the fault characteristic frequency are usually unknown in advance. For above reasons, it is necessary to effectively diagnose the fault and estimate the running state of spindle bearings, so as to recognize the principle of spindle bearing operation, optimize the bearing design, avoid unscheduled downtime and reduce the maintenance cost [4]–[7].

The temperature, acoustic emission (AE) and vibration signals of spindle bearings with different fault types and damage degrees can be obtained by using a variety of sensors.

46824

VOLUME 8, 2020

P. Xia *et al.*: Improved Underdamped Asymmetric Bistable SR Method and Its Application for Spindle Bearing Fault Diagnosis

IEEE*Access*

The specific fault diagnosis method is used to process the collected signals and diagnose the fault types. And the severity of bearing damage suitable indicators is evaluated by a suitable indicator. Finally, the maintenance decision is given. Temperature measurement is usually used as an auxiliary measurement method, because the temperature signal is only sensitive to serious bearing failure. AE measurement method can get a higher frequency range than vibration measurement method, and can avoid the influence of typical mechanical noise. In the analysis of rotating machinery system, although AE signal is more sensitive to the energy of incipient bearing fault, there is no extensive understanding and standard protocols on the relationship between the AE signal and bearing fault severity, which is not conductive to describing the development process of the bearing fault severity. Vibration signals in mechanical systems, which include impulse signals and periodic signals, often carry meaningful information about bearing failure, external interference and transmission path. Therefore, analyzing the vibration signal is an effective method for fault diagnosis of spindle bearings.

The traditional method of extracting fault-related transient vibration signals is to diagnose bearing faults by eliminating or filtering the noise [8]. However, the filtered noise may contain a lot of unexpected useful information. Regarding the SR mechanism, the noise is used for enhancing the fault-related signal and reducing the risk of losing the information of interest [9]. With continuous operation of the rotating spindle, rolling bearings will be damaged in different locations and extents. Research on this aspect, A. P .Pmpusunggu *et al.* [10] proposed an improved SR-based multi-noise tuned bearing condition monitoring method for the multi-fault diagnosis of the low-speed and light-load rolling bearings. For the fault diagnosis of centrifugal compressor blades, He *et al.* [11] proposed an improved bistable stochastic resonance method. In addition, Mba *et al.* [12] introduced a new condition monitoring and state classification system of gearboxes using SR method and hidden Markov models. Gunes *et al.* [14] indicated that the symmetric quartic potential well can be used as a low-pass filter for BPAM receivers. In the field of bearing fault diagnosis, several signal filtering methods based on SR have been studied [15]–[18]. Lu *et al.* [15] proposed an underdamped bistable SR (UBSR) algorithm for fault diagnosis of on-line bearing. The core part of the algorithm is an adaptive bistable nonlinear filter based on underdamped SR. Dong *et al.* [16] matched the nonlinear system, background noise and weak periodic signal by choosing the appropriate damping factor in the case of second-order parameter matching, thus producing an enhanced output. In order to diagnose incipient bearing faults, Qiao *et al.* [17] introduced an underdamped multi-scale SR (UMUSR) method and Xia *et al.* [18] proposed an underdamped periodic SR (UPSR) method for rolling bearing fault diagnosis. They indicated that the overdamped SR method is similar to a low-pass filter, but can hardly deal with multi-scale noise, so a high-pass filter is also needed. While underdamped SR method is shown as a non-linear bandpass

filter, which can suppress multi-scale noise more effectively. These results indicate that the under-damped SR is superior to over-damped SR in weak signal detection. Moreover, Qiao *et al.* [19] and Liu *et al.* [20] studied potential well asymmetry effect on overdamped asymmetric bistable SR (OABSR) under additive and multiplicative noise. And their results showed that the asymmetry can improve the enhancement ability of OABSR in weak feature extraction. Here we put forward an underdamped asymmetric SR (UABSR) method for spindle bearing fault diagnosis, in which the well-width asymmetric potential in [19], [20] was first applied in the field of mechanical fault diagnosis.

Besides, there are rare studies on SR-based fault diagnosis method for spindle rolling bearings in real practices. To ensure safe operation and maintain machining accuracy, slight changes require timely feedback and understanding during the operating state of the spindle bearings. The impact vibration signals contain lots of information related to bearing faults in the form of special frequencies caused by bearing defects. According to the classical analytical expressions and the geometrical structure of the bearing, the induced-frequency of the bearing corresponding to the local faults on each bearing element can be calculated. Nevertheless, the effects of environmental noise, in particular, impulsive noise from the spindle in a machine tool must be considered and relieved during chip processing. In addition, the fault locations of bearings are unknown in practical engineering applications, the fault frequency range for SR fault diagnosis cannot be determined in advance, and the commonly used Signal-to-Noise Ratio (SNR) [17], [18] in SR for enhancing the weak fault signal can hardly take effect if the fault frequency is unknown and pre-set. The weighted power spectrum kurtosis index [23] and spectral power amplification factor [24] can quantify the SR response, without knowing the prior information of bearing failure status. But they are particularly sensitive to the noise in vibration signals [25]. For evaluating the purity of the SR output signal, TDZC index [15] can directly reflect the regularity of the bearing fault signal without knowing the exact frequency of the target signal in advance. In order to reduce the impact of impulsive noise and achieve convenience in real practices, an improved UABSR method for spindle bearing fault diagnosis is proposed in this paper. Firstly, the fault characteristic frequency range of transient impulses is determined by using Infogram method which can avoid the influence of impulsive noise. Secondly, the TDZC index is adopted in the UABSR method to directly reflect spindle bearing fault characteristics without knowing the exact fault characteristic frequency in advance. Besides, the QGAs and the fourth-order Runge-Kutta algorithm are combined to obtain the optimal system parameter, asymmetric ratio, damping factor and rescaling factor of the new UABSR model simultaneously. In other words, improved UABSR can be regarded as a nonlinear bandpass filter. By adjusting the parameters of the UABSR model, the signal of interest which is severely masked by the large background noise can be amplified.

IEEE Access

P. Xia *et al.*: Improved Underdamped Asymmetric Bistable SR Method and Its Application for Spindle Bearing Fault Diagnosis

The rest of this study is organized as follows. Section II reviews the theoretical foundation of the improved UABSR method. The simulation verification and experimental verification are respectively performed in Section III and Section IV. And Section V concludes the paper.

II. THEORETICAL FOUNDATION

A. UNDERDAMPED SCALE-TRANSFORMATION STOCHASTIC RESONANCE THEORY

Underdamped SR is a nonlinear physical phenomenon where the nonlinear systems have a specific performance for transforming noise energy to enhance the weak bearing fault signals. The classic underdamped SR based on the nonlinear system $U_{i0}(x)$ by Gaussian white noise $N(t)$ and the periodic signal $S_0(t) = A_0 \sin(2\pi f_{d0}t + \varphi_0)$ is governed by

$$\frac{d^2x}{dt^2} = -\frac{dU_{i0}(x)}{dx} - \beta_0\frac{dx}{dt} + A_0\sin(2\pi f_{d0}t + \varphi_0) + N(t)$$

$$(1)$$

where x is the trajectory of a weak periodic particle, the parameters of the potential $U_{i0}(x)$ are the smaller system parameters, which scope is usually set to [0, 3]. β_0 is the damping factor of the system. A_0, φ_0 respect the weak amplitude and phase of the periodic impact signal, respectively. The driving frequency f_{d0} is much smaller than 1, so periodic low-frequency signal can be enhanced by Eq. (1).

For the high-frequency fault signal of spindle rolling bearing $S(t) = A\sin(2\pi f_d t + \varphi)$, the underdamped bistable SR model can be written as

$$\frac{d^2x}{dt^2} = -\frac{dU_i(x)}{dx} - \beta\frac{dx}{dt} + A\sin(2\pi f_d t + \varphi) + D\xi(t) \quad (2)$$

where $U_i(x)$ is a bistable potential. Herein, the much larger system parameters of $U_i(x)$ are positive real numbers. β is the damping factor of the underdamped system. $A, f_d > 1$, and φ represents the amplitude, driving frequency and phase of the periodic impact signal, respectively. D and $\xi(t)$ represents the noise intensity and additive Gaussian white noise.

Introducing the scale transformation factor m and substitution variables $g(\delta) = \sqrt{b/a}x(t)$, $\delta = mt = at$, to realize large scale transform. After transformation, Eq. (2) can be rewritten:

$$\frac{d^2g}{d\delta^2} = -\frac{1}{m}\frac{dU_i(g)}{d\delta} - \frac{\beta}{m}\frac{dg}{d\delta}$$
$$+ \sqrt{\frac{b}{m^5}}A\sin(2\pi\frac{f_d}{m}\delta + \varphi) + \sqrt{\frac{b}{m^5}}D\xi(\frac{\delta}{m}) \quad (3)$$

Introducing the variables substitutions,

$$\frac{1}{m}\frac{dU_i(g)}{d\delta} = \frac{dU_{i*}(g)}{d\delta}, \frac{\beta}{m} = \beta_*,$$

$$\frac{f_d}{m} = f_{d*}, \sqrt{\frac{b}{m^5}}A = A_*, \sqrt{\frac{b}{m^5}}D = D_*,$$

the auxiliary expression can be rewritten as

$$\frac{d^2g}{d\delta^2} = -\frac{dU_{i*}(g)}{d\delta} - \beta_*\frac{dg}{d\delta} + A_*\sin(2\pi f_{d*}\delta + \varphi) + D_*\xi(\frac{\delta}{m})$$

$$(4)$$

where the system parameters of the $U_{i*}(g)$, β_* and f_{d*} are all the larger parameters. By comparing Eq. (2) to Eq. (4), it is to find that the f_{d*} is converted into $1/m$ times of the original signal frequency and their dynamic properties are identical in essence. Moreover, the detection range of target frequency can be adjusted by changing the rescaling factor m. Furthermore, the system parameters, the asymmetric ratio, the damping factor and the rescaling factor can be selected and optimized by QGAs [26], and the system output shown as Eq. (4) can be solved using the fourth-order Runge-Kutta algorithm.

B. UNDERDAMPED ASYMMETRIC BISTABLE SR INDUCED BY WELL-WIDTH ASYMMETRY

The conventional bistable $U_0(x)$ and asymmetric bistable potential $U_i(x)$ with three types are described as [19]:

$$U_0(x) = -ax^2/2 + bx^4/4 \quad (5)$$

$$U_i(x) = \begin{cases} -ax^2/2 + bx^4/4 & x \geq 0, \\ -aA_ix^2/2 + bB_ix^4/4 & x < 0, \end{cases} \quad (6)$$

where $i = 1, 2, 3, A_1 = B_1 = \alpha, A_2 = 1/\alpha^2, B_2 = 1/\alpha^4, A_3 = 1, B_3 = 1/\alpha^2$, the asymmetric ratio $\alpha > 0$ and the system parameters $a, b \in [0, 3]$. For a certain range of the α in a potential system, the larger the value of α, the greater the degree of the asymmetry. Fig. 1 (a) shows the traditional bistable potential where $a = 1$ and $b = 1$. And Fig. 1 (b), (c) and (d) shows asymmetric bistable potentials under different asymmetric ratio α where $a = 1$ and $b = 1$. From Eq. (3) and Fig. 1, it can be obtained that the shape of the right potential well located at $x > 0$ is unaffected by the asymmetric ratio α in all three kinds asymmetric potentials. For the potential $U_1(x)$ shown in Fig. 1(b), the stable and unstable states are at $x_\pm = \pm\sqrt{a/b}$ and $x_u = 0$, respectively.

In addition, the well width obviously remains as $2\sqrt{a/b}$. So, only the depth of the left well $\alpha a^2/(4b)$ is possible to be adjust by α. Therefore, $U_1(x)$ can just reflect the influence of asymmetric well depth on the bistable SR. In a similar way, only the influence of well-width asymmetry on SR can be explored by $U_2(x)$. Besides, in $U_3(x)$ both the depth and the width of the left well depend on α, which can study the effect of both well-width and well-depth asymmetry on the bistable SR.

In this paper, the method of underdamped stochastic resonance induced by well-width asymmetric bistable potential is used to diagnose spindle bearing faults. The potential function of the well-width asymmetry type, that is, the case of Eq. (3) when $i = 2$. Substitute $A_2 = 1/\alpha^2$, $B_2 = 1/\alpha^4$ into Eq. (3),

$$U_2(x) = \begin{cases} -ax^2/2 + bx^4/4 & x \geq 0, \\ -ax^2/2 + bx^4/4\alpha^2 & x < 0, \end{cases} \quad (7)$$

After calculation, it can be derived from Eq. (7) that in $U_2(x)$ the depth of the two wells remain at $a^2/(4b)$, and the
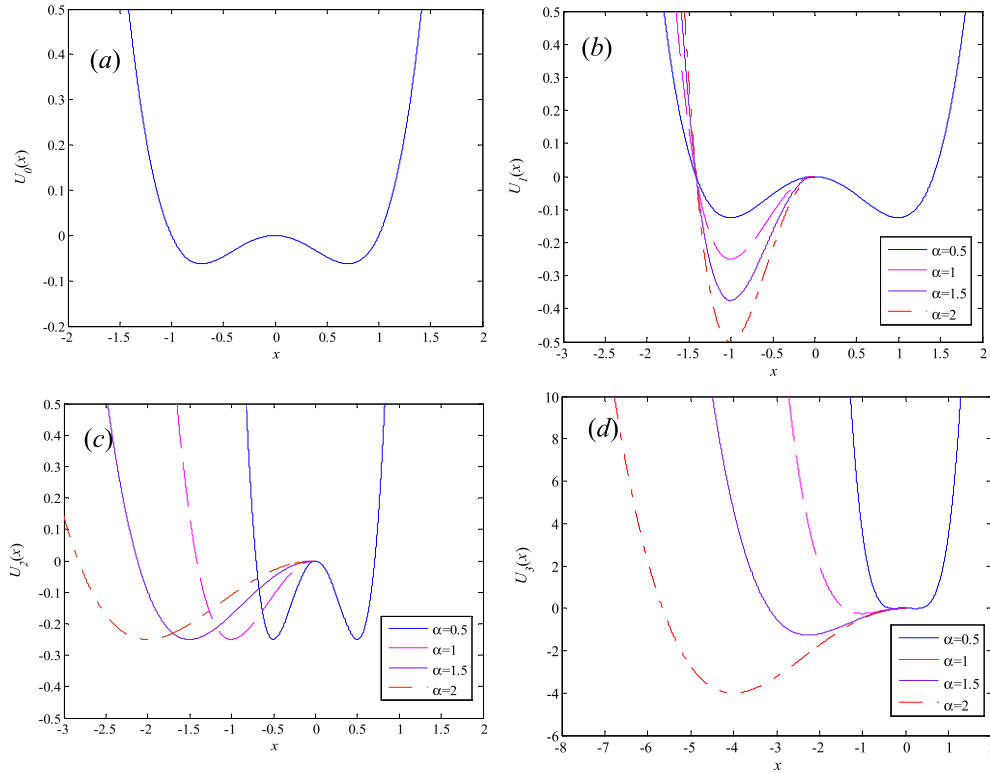
P. Xia *et al.*: Improved Underdamped Asymmetric Bistable SR Method and Its Application for Spindle Bearing Fault Diagnosis

IEEEAccess

FIGURE 1. Traditional bistable potential and asymmetric bistable potential where $a = 1$ and $b = 1$: (a) traditional bistable potential $U_0(x)$, (b) well-depth asymmetrical potential $U_1(x)$, (c) well-width asymmetrical potential $U_2(x)$ and (d) well-depth and well-width asymmetrical potential $U_3(x)$.

two stable states lie at $x_- = -\alpha\sqrt{a/b}$ and $x_+ = -\sqrt{a/b}$, respectively. Hence, $U_2(x)$ attempts to investigate the effect of well-width asymmetry on SR alone. Eq. (2) can be divided into two first-order differential equations as Eq. (8).

$$\frac{dx}{dt} = z, \quad \frac{dz}{dt} = \begin{cases} ax - bx^3 - \beta z + in(t) & x \geq 0 \\ ax - bx^3/\alpha^2 - \beta z + in(t) & x < 0 \end{cases} \quad (8)$$

where $in(t) = A\sin(2\pi f_d t + \varphi) + D\xi(t)$. Eq. (8) can be calculated using Eq. (9).

$$\begin{cases} x_1 = -U_2'(x_{[n-1]}) - \beta z_1 + in_{[n-1]} \\ z_1 = z_{[n-1]} \\ x_2 = -U_2'(x_{[n-1]} + z_1 h/2) - \beta z_2 + (in_{[n-1]} + in_{[n]})/2 \\ z_2 = z_{[n-1]} + x_1 h/2 \\ x_3 = -U_2'(x_{[n-1]} + z_2 h/2) - \beta z_3 + (in_{[n-1]} + in_{[n]})/2 \\ z_3 = z_{[n-1]} + x_2 h/2 \\ x_4 = -U_2'(x_{[n-1]} + z_3 h) - \beta z_4 + in_{[n]} \\ z_4 = z_{[n-1]} + x_3 h \\ z_{[n]} = z_{[n-1]} + (x_1 + 2x_2 + 2x_3 + x_4)h/6 \\ x_{[n]} = x_{[n-1]} + (z_1 + 2z_2 + 2z_3 + z_4)h/6 \end{cases} \quad (9)$$

where h is the calculation step, and $x_{[n]}$, $z_{[n]}$, and $in_{[n]}$ are the discrete forms of $x(t)$, $z(t)$, and $in(t)$, respectively.

Eq. (9) is expressed by the following Eq. (10):

$$\begin{aligned} x_{[n]} = &\sum_{i=1}^{3}\sum_{l=1}^{2} \Omega_{i,l} \cdot in_{[n-l]}^i + \sum_{j=1}^{9} N_j \cdot x_{[n-1]}^j \\ &+ \sum_{k=1}^{3} \eta_k \cdot z_{[n-1]}^k + \sum_{i=1}^{2}\sum_{j=1}^{6} \Gamma_{i,l} \cdot in_{[n-l]}^i x_{[n-1]}^j \\ &+ \sum_{j=1}^{6}\sum_{k=1}^{2} \Pi_{j,k} \cdot x_{[n-l]}^j z_{[n-1]}^k \\ &+ in_{[n-1]} z_{[n-1]} + in_{[n-1]} x_{[n-1]}^3 z_{[n-1]} \end{aligned} \quad (10)$$

where $\Omega_{i,l}$, N_j, η_k, $\Gamma_{i,l}$ and $\Pi_{j,k}$ are coefficients dominated by parameters a, b, α, β and h.

From Eq. (10), we can conclude that the output $x_{[n]}$ of UABSR is determined by the input $in_{[n-l]}$ and previous output $x_{[n-1]}$, $z_{[n-1]}$ and it can be regarded as a specific noise-enhanced nonlinear filter similar to a classical noise-suppression linear IIR filter [11]. The equation of IIR filter is shown as Eq. (11).

$$\hat{x}_{[n]} = -\sum_{k=1}^{L} a_k \hat{x}_{[n-k]} + \sum_{k=0}^{M} b_k \cdot in_{[n-k]} \quad (11)$$

where a_k and b_k are filter coefficients.

By adjusting the parameters of the non-linear under-damped well-width asymmetric bistable system, the signal of

IEEE *Access*

P. Xia *et al.*: Improved Underdamped Asymmetric Bistable SR Method and Its Application for Spindle Bearing Fault Diagnosis
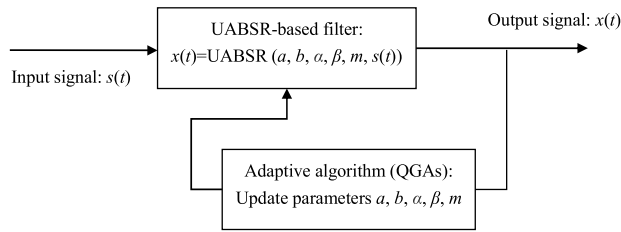

FIGURE 2. Framework of the UABSR-based filter.

interest which is seriously masked by the large background noise can be amplified. The UABSR-based filter as shown in Fig. 2 is used for signal denoising and the signal of interest can be implemented by adjusting parameter pairs (a, b, α, β, m, which are positive real numbers) of the underdamped asymmetrical bistable potential.

C. PARAMETER SELECTION FOR ADAPTIVE UABSR-BASED FILTER AND ITS PARAMETER OPTIMIZATION

The acquired mechanical vibration signals as the input through the UABSR-based filter using the QGAs [26] to find the optimal parameters (a^*, b^*, α^*, β^*, m^*) and output the purified bearing fault signals from the input signal to an extreme. First of all, a suitable indicator is needed for constructing the optimal UABSR-based filter.

In view of the operation environment of spindle bearings and their prior knowledge [17], [18], [23]–[25], TDZC index [15] is used for parameters optimization of the UABSR-based filter. Thus, the calculation algorithm of the TDZC index is given as follow:

The time intervals between the successive time domain zero crossing points (TDZCP) are related to the frequencies present in the discrete time domain signal, and the statistical regularity of TDZCP can be used to characterize the purity of the UABSR-filtered signal.

Step 1: Calculate the UABSR-based filter output using Eq. (9) and then obtain $x_{[n]}, n \in \{1, 2, \ldots, N\}$, where N is the length of the time series.

Step 2: Calculate the TDZCP of $x_{[n]}$ and obtain $TDZCP(k)$, $k \in \{1, 2, \ldots, K, K \leq N\}$, where K is expressed as the number of TDZCP.

Step 3: Calculate the differences between adjacent $TDZCP(k)$ as: $TDZC(k) = TDZCP(k + 1) - TDZCP(k)$, $k \in \{1, 2, \ldots, K - 1\}$.

Step 4: Computed the purity of the signal, that is, the formula of the TDZC index is computed as:

$$TDZC = {}^1/\!K - 1 \sum_{k=1}^{K-1} \left| TDZC(k) - {}^1/\!K-1 \sum_{k=1}^{K-1} TDZC(k) \right|,$$
$$k \in \{1, 2, \ldots, K - 1\}. \quad (12)$$

Compared with SNR [18], the TDZC index is inversely correlated with the changing trend of optimization parameters [15]. Hence, the objective function of the optimal output can be achieved as follows:

$$(a^*, b^*, \alpha^*, \beta^*, m^*) = \arg \min TDZC(a, b, \alpha, \beta, m) \quad (13)$$

where (a^*, b^*, α^*, β^*, m^*) indicate the corresponding optimal parameter pairs of the UABSR-based filter.

A commonly used parameter optimization algorithm, QGAs [17], is applied for accelerating the parameter searching speed and obtaining the optimal system parameter, asymmetric ratio, damping factor and rescaling factor. Using the QGAs, (a^*, b^*, α^*, β^*, m^*) that produce the minimum TDZC index can be obtained.

D. IMPROVED UABSR METHOD FOR SPINDLE BEARING FAULT DIAGNOSIS

In the actual engineering environment of the spindle bearing, impulsive noise is inevitable and will affect the effectiveness of bearing fault detection, but the general SR method lacks the basis of removing it. Transient signals contain lots of fault information in the form of bearing fault characteristic frequency. In order to effectively extract the bearing fault, it is necessary to determine the resonance band of fault bearing. According to the classical formula and the geometrical parameters of the bearing, the fault characteristic frequency of each bearing element can be calculated. However, the fault location of bearing is unknown in engineering practice and the fault frequency range for SR-based weak signal detection method is not able to predict in advance. At this time, if the indicators, e.g., SNR [18], weighted power spectrum kurtosis [23] and spectral power amplification [24] are used to determine the occurrence of stochastic resonance, the results will not only be affected by impulsive noise, but also may cause misjudgment or difficult to judge.

In view of the industrial environment, the improved UABSR method for spindle bearing fault diagnosis are proposed and summarized in Fig. 3. The detailed procedures are described below.

Step 1: Infogram method is performed on the original fault vibration signal of spindle bearing to obtain the corresponding suitable frequency band range of the UABSR-based bandpass filter. To be specific, after performing Inforgram method on the vibration signal, the SE (squared envelope), SES (squared envelope spectrum) and average infograms are illustrated. The SES infogram is insensitive to impulsive noise and can clearly reveal the repetitive fault transient signals [21]. In addition, the joint analysis of SE and SES information diagrams makes it possible to distinguish different transient events in practical applications. Hence, Infogram method can resist the influence of impulsive noise and clearly give the band-pass filtering frequency range of the bearing fault transient signal.

Step 2: The techniques of the Hilbert envelope analysis and band-pass filtering are performed to pretreat the original vibration signal of fault bearings collected by an acceleration sensor.

Step 3: Preset the initial parameters include the population size M, the length of each binary variable L, the terminal generation size $T_{\max}$ and the range of the parameters of a, b, α, β, m before executing the QGAs [17], [26] and,

P. Xia *et al.*: Improved Underdamped Asymmetric Bistable SR Method and Its Application for Spindle Bearing Fault Diagnosis
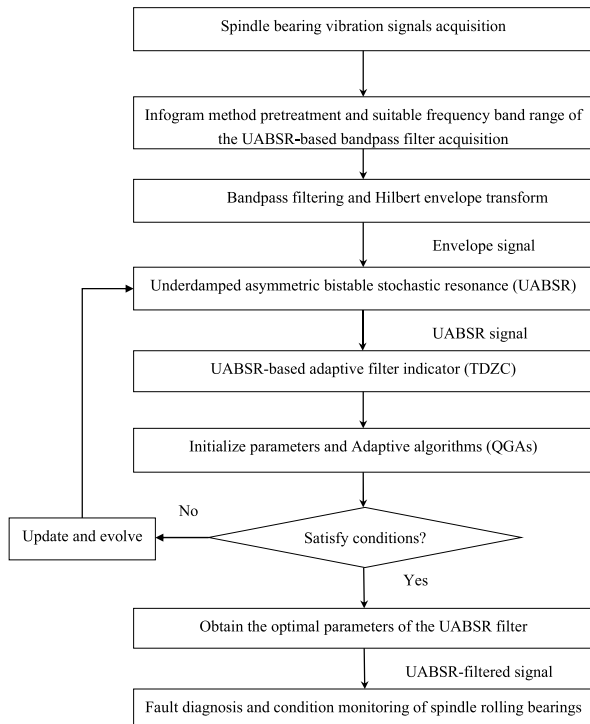
IEEE *Access*

FIGURE 3. Flowchart of the improved UABSR spindle bearing fault diagnosis method.

in order to obtain the $(a^*, b^*, \alpha^*, \beta^*, m^*)$, the default parameter values and the initial search range are as follows.

(1) Population size $M = 40$.

(2) Length of each binary variable $L = 20$.

(3) Terminal generation size $T_{\max} = 40$.

(4) Variation ranges for system parameters $a \in (0, 3], b \in (0, 3]$.

(5) Variation ranges for asymmetric ratio $\alpha \in (0.1, 5]$.

(6) Variation ranges for damping constant $\beta \in [0, 1]$.

(7) Variation ranges for rescaling factor $m \in (0, 1000]$.

To obtain an universal range for diagnosing spindle bearing faults, according to UABSR theory we initialize the search ranges of system parameters and the asymmetric ratio to $a \in (0, 3], b \in (0, 3]$ and $\alpha \in (0.1, 5]$. Generally considered, the range of the damping factor is $\beta \in [0, 1]$. To satisfy the small-parameter requirement of UABSR ($f \ll 1$Hz), the rescaling factor m is initialized as $m \in (0, 1000]$.

Step 4: QGA is used to optimize the parameters of UABSR model. Based on quantum theory and quantum computation, the algorithm uses quantum bits to realize individual coding, and then searches for the optimal solution of the individual in each iteration through quantum revolving gate operation. A qubit (quantum bit) is the smallest information unit of a two-state quantum system. In QGA, instead of binary, numeric, or symbolic representation, the qubit is used to store and represent one gene. Then, the initial quantum population $P(t) = \{p_1^t, p_2^t, \cdots, p_m^t\}$ is generated randomly, in which the tth generation of the ith individual p_i^t is encoded by qubit probability, and the probability amplitudes of the whole

chromosomes is equal to $1 / \sqrt{2}$. Besides, the individuals of the population $P(t)$ is measured and the binary solution set $Q(t)$ is obtained.

Step 5: The envelope signal is input into Eq. (8), and the corresponding output signal is calculated by the fourth-order Runge-Kutta method. To ensure a good distinction between fault characteristic frequencies and the disturbances, TDZC index [15] is introduced to the proposed UABSR method. The TDZC index, which can directly reflect spindle bearing fault characteristics without knowing the exact fault characteristic frequency, is expected to be suitable as the indicator of the improved UABSR method. The TDZC index values of each definite solution in $Q(t)$ are calculated, and the optimal solution and corresponding TDZC index are recorded.

Step 6: Update the Q-bits of the chromosome by quantum rotation gates [26], and evolve individuals of $Q(t)$ to a new population $Q(t+1)$. In QGA, the rotation gate is an important updating method for generating the probability amplitude of quantum states.

Step 7: Termination condition judgement. Output the optimum solution of parameter pairs $(a^*, b^*, \alpha^*, \beta^*, m^*)$ of the UABSR model and the corresponding optimum value of TDZC index when the iteration times of the QGAs reach to the pre-defined maximum iteration, otherwise, continue Step 6 to find the optimal solution.

Step 8: Set the optimal parameter values according to the $(a^*, b^*, \alpha^*, \beta^*, m^*)$, and then put the envelope signals obtained by Step 3 into the calculation formula of the TDZC index for calculating its value. After that, the optimized signal enhancement results are acquired to extract weak fault characteristic frequency and diagnose incipient spindle bearing faults.

In other words, the improved UABSR can be regarded as a nonlinear bandpass filter. By adjusting the parameters of the non-linear asymmetry bistable system, the signal of interest which is seriously masked by the background noise can be amplified. Firstly, before the application of the UABSR method, the frequency range of repetitive transient of bearing fault signal is obtained by Infogram. Then, the improved UABSR spindle bearing fault diagnosis method of parameter optimization based on the TDZC index is applied in this frequency range by the principle of scale transformation.

III. SIMULATION VERIFICATION
A series of repetitive transient signals generated by faulty the spindle rolling bearing in chip processing environment are simulated by the following model [22].

$$x(t) = H \sin(2\pi f_n t) \cdot \exp\{-d[t - n(t)/f_d]^2\} + I(t) + N(t) \tag{14}$$

where $n(t) = f_d \times t$ indicates the number of the fault impulses, the amplitude of the impulses $H = 0.8 - 1.6$m $\cdot$ s^{-2}, the resonance frequency $f_n = 2000$ Hz, the attenuation coefficient $d = 600$, the fault characteristic frequency $f_d = 50$ Hz, the sampling frequency and sampling time are set to
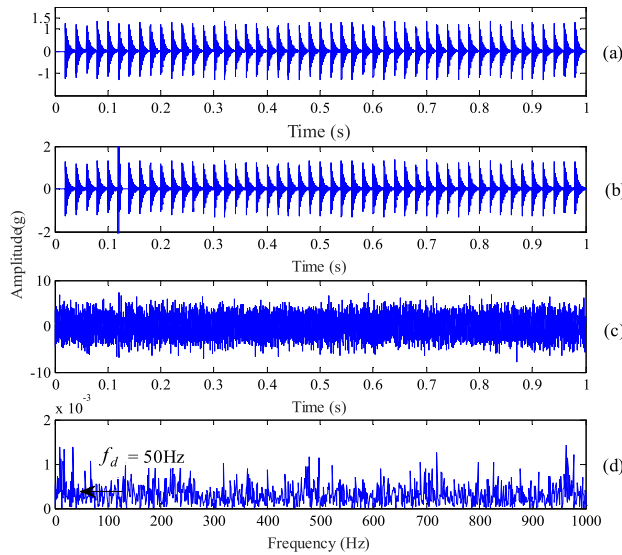
IEEE *Access*

P. Xia *et al.*: Improved Underdamped Asymmetric Bistable SR Method and Its Application for Spindle Bearing Fault Diagnosis

FIGURE 4. Time domain waveform and frequency spectrum of simulated signal: (a) Simulated fault signal of spindle bearing, (b) fault bearing signal with the impulsive noise, (c) fault bearing signal with the impulsive noise and white noise where D = 2 and (d) the Hilbert envelope frequency spectrum of Fig. 4(c).

f_s = 12000Hz and t = 1s. $I(t)$ stands for an impulsive noise, $N(t)$ represents Gaussian white noise and satisfies the statistical conditions as follow:

$$\begin{cases} \langle N(t) \rangle = 0 \\ \langle N(t)N(t+\tau) \rangle = 2D\delta(\tau) \end{cases} \quad (15)$$

where D stands for the intensity of additive Gaussian white noise.

Fig. 4(a) shows the simulated spindle bearing fault signal. Similar to the response of a single-degree-of-freedom system, the impulsive noise $I(t)$ with amplitude 8 m · s^{-2}, resonance frequency 5000 Hz, and bandwidth 800 Hz to a Dirac impulse is added in Fig. 4(a) at 0.12 s. So, the simulated spindle bearing fault signal with the impulsive noise is plotted in Fig. 4(b). After adding the white Gaussian noise $N(t)$ with D = 2, the mixed signal and its Hilbert envelope frequency spectrum are shown in Fig. 4(c) and Fig. 4(d), respectively. Due to the influence of background noise, the envelope frequency spectrum shown in Fig. (4) is very complicated and can basically be used to simulate the actual operating environment. It can be seen that the bearing fault characteristic frequency shown in Fig. 4(d) are almost buried in the background noise.

Infogram method is performed on the simulated signals shown in Fig. 4(c). Then, the corresponding SE, SES and average infograms are displayed in Fig. 5(a), (b) and (c). The joint analysis of SE and SES information diagrams makes it possible to distinguish different transient events in practical applications. In particular, the SES infogram is insensitive to impulsive noise and repetitive transients can be detected even in the presence of the strong impulsive noise [21]. The SE infogram (Fig. 5(a)) shows that the high value of level 5 is about 5000 Hz. Since there is no equivalence in
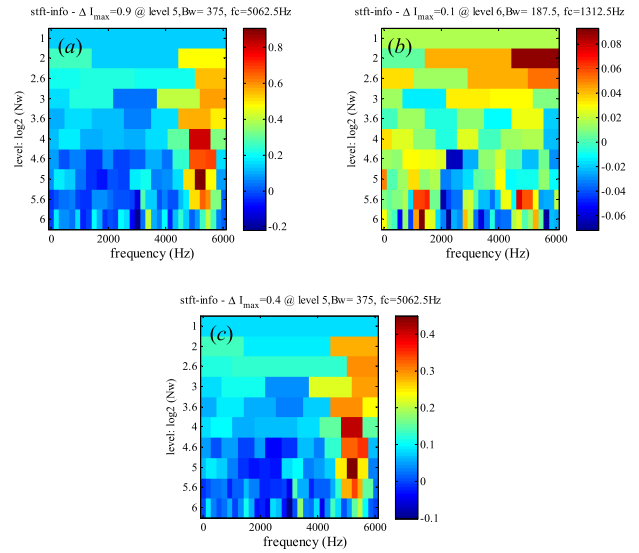

FIGURE 5. Analysis of the simulated fault signal of spindle bearing with the impulsive and white noise shown in Fig. 4(c): (a) SE infogram, (b) SES infogram, (c) average infogram.
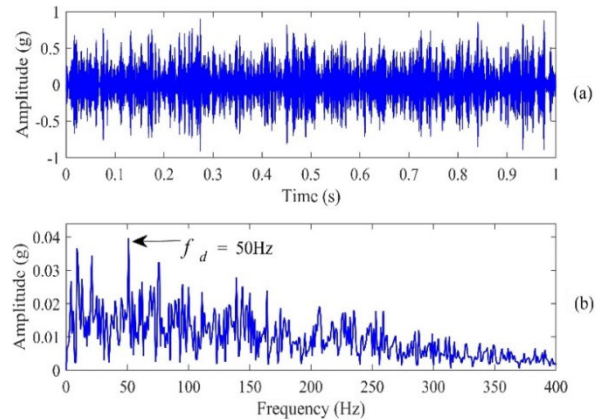

FIGURE 6. Fault characteristic frequency extraction results of the simulation signal using the improved UABSR method: (a) time domain waveform and (b) its frequency spectrum.

the SES infogram (Fig. 5(b)), the corresponding event should be the impulsive noise. And in SES infogram shows that the high values below level 5 around 1350 Hz is expected to be the fault transients. Hence, through the analysis of Fig. 5(a) and (b), we roughly choose [1050, 1750] Hz as the suitable frequency band range of the bandpass filter for the simulation signal. Then, QGAs are used to optimize the parameters pairs (a, b, α, β, m) of the improved UABSR method with the asymmetric bistable potential shown in Eq. (7). According the improved UABSR method in Section 2.4, the adaptive diagnosis result of the proposed method is displayed in Fig. 6 with the optimal parameter pair $(a, b, \alpha, \beta, m) = (2.9590, 1.4251, 0.4593, 0.5685, 457.2348)$. For comparison, the corresponding results of the SES infogram and the original UABSR method are also displayed in Fig. 7 and 8. Compared with the improved UABSR method, the original UABSR method uses high-pass filtering
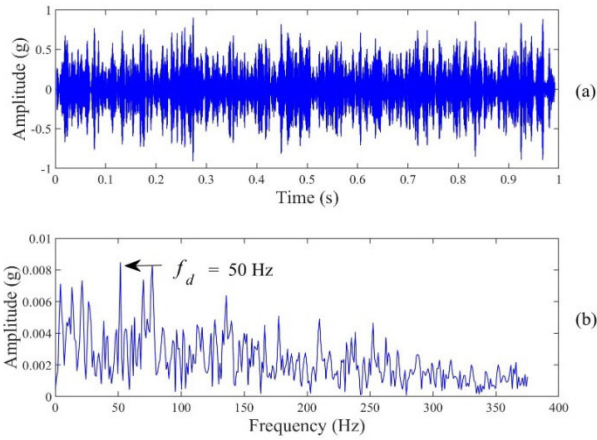
P. Xia *et al.*: Improved Underdamped Asymmetric Bistable SR Method and Its Application for Spindle Bearing Fault Diagnosis

IEEE*Access*

FIGURE 7. Fault characteristic frequency extraction results of the simulation signal using the SES Infogram method: (a) the filtered time domain waveform and (b) its frequency spectrum of the squared filtered signal.
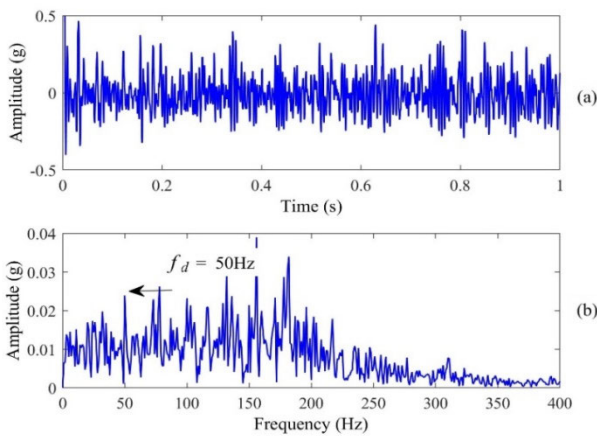

FIGURE 8. Fault characteristic frequency extraction results of the simulation signal using the original UABSR method: (a) time domain waveform and (b) its frequency spectrum.

to preprocess the original vibration signal. Although the fault characteristic frequency (50 Hz) in Fig. 7 and 8 is extracted from the fault signal with the impulsive noise and white noise, there still exists strong interference around the fault characteristic frequency. However, the amplitudes of the fault characteristic frequency 50 Hz and its harmonics frequency in Fig. 6 are higher than that in Fig. 7 and 8. The results show that the proposed improved UABSR method is reliable and effective.

IV. EXPERIMENTAL VERIFICATION

In this section, two bench tests of actual spindle bearing fault have been employed to evaluate the effectiveness of the improved UABSR method in fault diagnosis of spindle rolling bearings.

A. FAULT DIAGNOSIS OF SPINDLE BEARING WITH THE ARTIFICIAL OUTER RACE DAMAGE

The improved UABSR method is used for fault characteristic extraction and damage degree assessment of the spindle bearing outer-ring defects with three different levels.
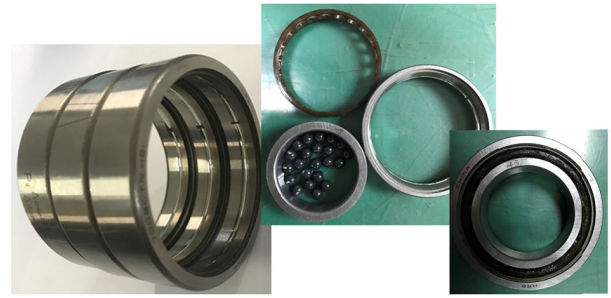

FIGURE 9. Outer race of hybrid ceramic ball bearing with three fault sizes, the decomposition and combination diagrams of the tested spindle bearing.
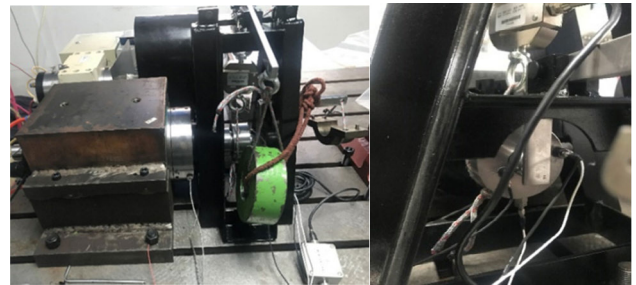

FIGURE 10. Experimental device and its acquisition arrangement.

TABLE 1. Geometric parameters of hrb 7008ctn/p4hq1.

Symbol	Component	Size and value
D_{outer}	outer ring diameter	68 mm
D_{inner}	inner ring diameter	40 mm
H	bearing width	15 mm
N	Number of balls	16
D_{ball}	Ball diameter	7.938 mm
α	Initial contact angle	15°
ω	outer ring angular velocity	1200 rpm

Hybrid ceramic angular contact ball bearings (HRB 7008 CTN/P4HQ1) are installed each time in the test device, as shown in Fig. 10. Fig. 9 shows the defective outer race of spindle bearing with the different fault width (0.6mm, 1.2mm and 1.8mm) and with the same fault depth (0.6 mm). Detailed parameters of test bearings are shown in Table 1. And the decomposition and combination diagrams of the four main components of the test bearing are also shown in Fig. 9. Four accelerometers are mounted on the bearing housing and their positions are shown in Fig. 10. Two accelerometers for measuring radial vibration of ball bearings are mounted vertically on the bearing seat. The other two accelerometers for measuring axial vibration are mounted on the housing, which is located near and away from the center of the shaft, respectively. The radial load of 118 N and the axial load of 25 N are applied to the test bearing. NI data acquisition card of PXI-4498 is used to collect bearing vibration data. The sampling rate of NI data acquisition device is 10,000 samples
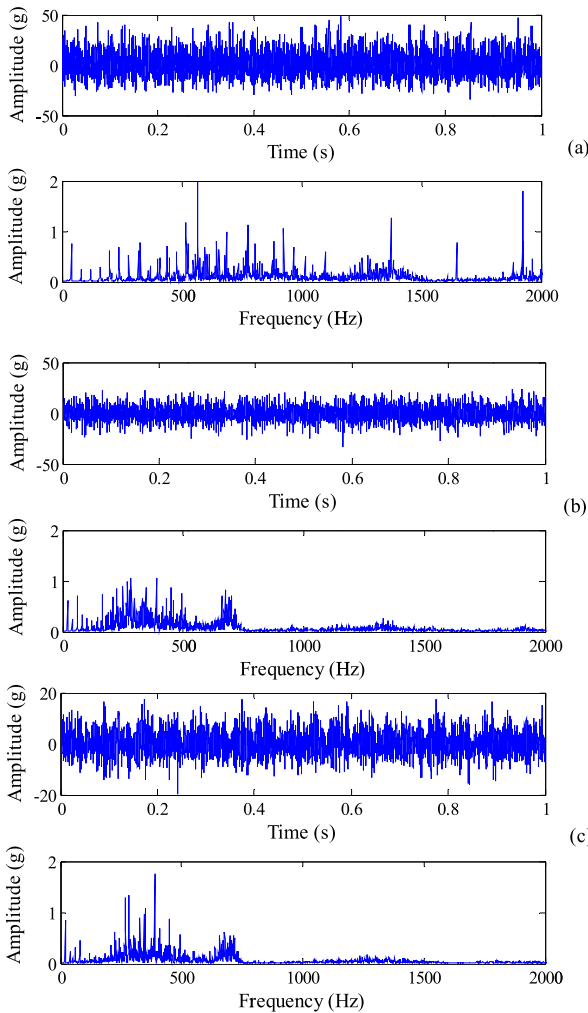
FIGURE 11. Time domain waveform and Hilbert envelope frequency spectrum of original vibration signal of experimental spindle bearing with outer-ring faults: (a) 0.6mm fault width, 0.6mm fault depth, (b) 1.2mm fault width, 0.6mm fault depth and (c) 1.8mm fault width with the same 0.6mm fault depth.

FIGURE 12. Analysis of the vibration signal of spindle bearing with an outer race fault (1.2mm fault width, 0.6mm fault depth): (a) SE infogram, (b) SES infogram, (c) average infogram of the signal in Fig. 11(b).

FIGURE 13. Fault characteristic frequency extraction results of the fault bearing vibration signal (outer-ring fault with 1.2mm fault width and 0.6mm fault depth) using the improved UABSR method: (a) Output time domain waveform and (b) its frequency spectrum.

per second, each sampling time is 1 s. The vibration signals in the radial bearing area are taken as the research data. The rotational speed of the shaft is about 1200 rpm. And the outer-ring fault characteristic frequency of the test spindle rolling bearing is about 165 Hz. The time domain waveforms and Hilbert envelope frequency spectra of vibration signals with three fault degrees are shown in the Fig. 11(a)-(c). However, fault features are completely covered by noise components.

The proposed improved UABSR method is used to evaluate the fault degree of the three kinds of artificial outer ring defects. As an example, the infogram method are performed on the vibration signals of spindle bearing with fault width of 1.2 mm. The high values of the infograms including SE, SES and average infogram for several regions are displayed in Fig. 12 (a)-(c). It is possible to distinguish different transient events in the presence of strong impulsive noise and independently of their rate of repetitions through the joint analysis of SE and SES infograms. Especially,
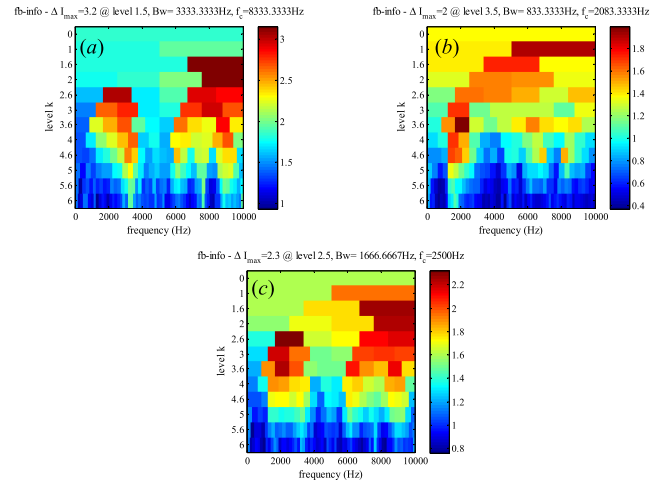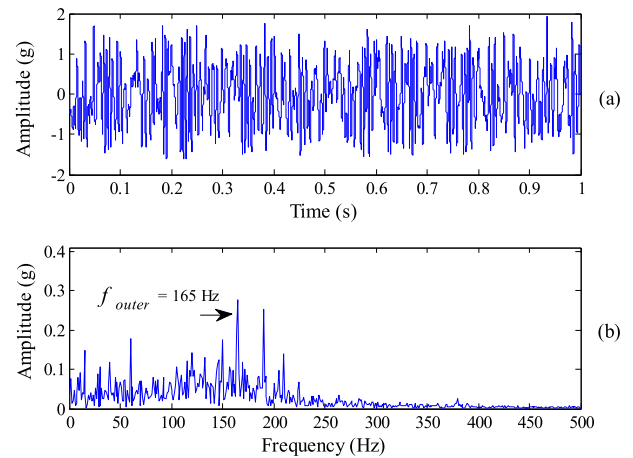
the SES infogram can resist impulsive noise and detect cyclostationarity. Through the analysis of Fig. 12, we choose [1250, 2916] Hz as the suitable frequency band range of the bandpass filter for this fault signal. Then, QGAs are used to optimize the parameters pairs (a, b, α, β, m) of the proposed UABSR method with the asymmetric bistable potential shown in Eq. (7). According Section 2.4, the adaptive diagnosis result of the improved UABSR method is displayed in Fig. 13 with the optimum parameters $(a, b, \alpha, \beta, m) = (0.9883, 0.8103, 4.4487, 0.5462, 370.3486)$. For a fair comparison, the corresponding results of the SES infogram and the original UABSR method (which is performed by the high-pass filtering) are also displayed in Fig. 14 and 15, respectively. Although the fault characteristic frequency in Fig. 14 and 15 (165 Hz) is extracted from the impact signal with the background noise, there still exists strong interference around the fault characteristic frequency.
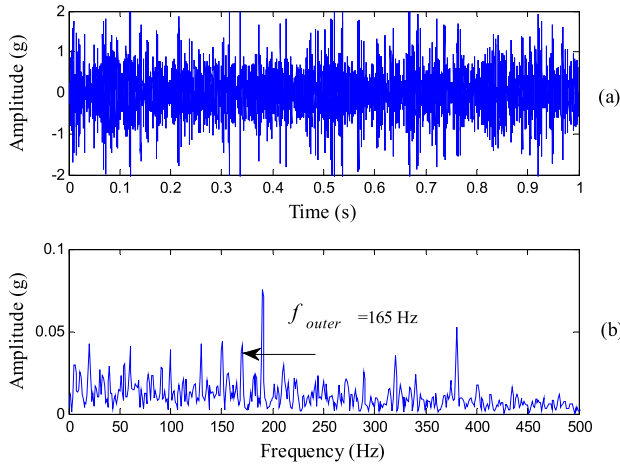
P. Xia *et al.*: Improved Underdamped Asymmetric Bistable SR Method and Its Application for Spindle Bearing Fault Diagnosis

IEEE*Access*

FIGURE 14. Fault characteristic frequency extraction results of the fault bearing vibration signal (outer-ring fault with 1.2mm fault width and 0.6mm fault depth) using the SES Infogram method: (a) the filtered time domain waveform signal and (b) its frequency spectrum.
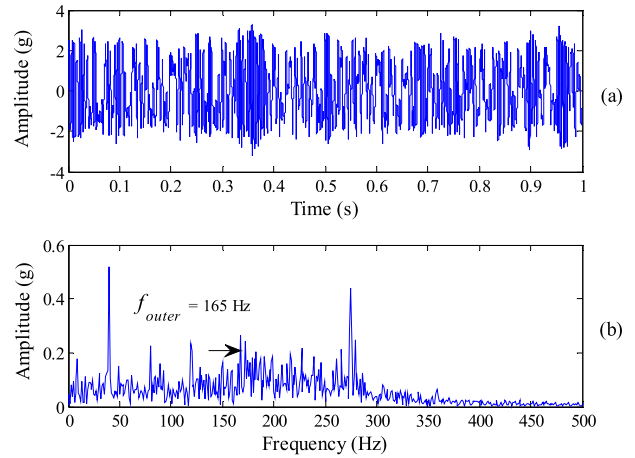

FIGURE 15. Fault characteristic frequency extraction results of the fault bearing vibration signal (outer-ring fault with 1.2mm fault width and 0.6mm fault depth) using the original UABSR method: (a) time domain waveform signal and (b) its frequency spectrum.

FIGURE 16. Fault characteristic frequency extraction results of the fault bearing vibration signal (outer-ring fault with 0.6mm fault width and 0.6mm fault depth) using the improved UABSR method: (a) Output time domain waveform and (b) its frequency spectrum.
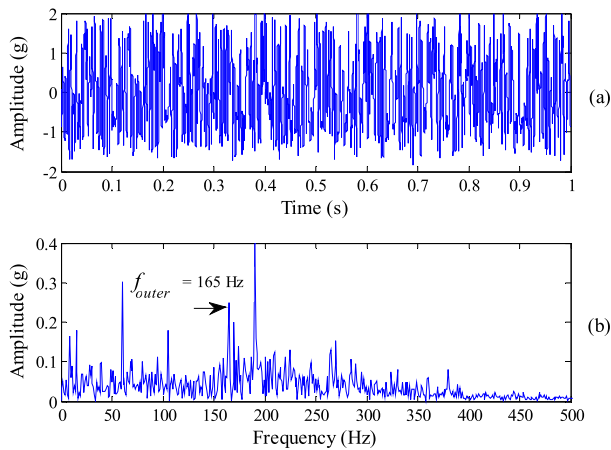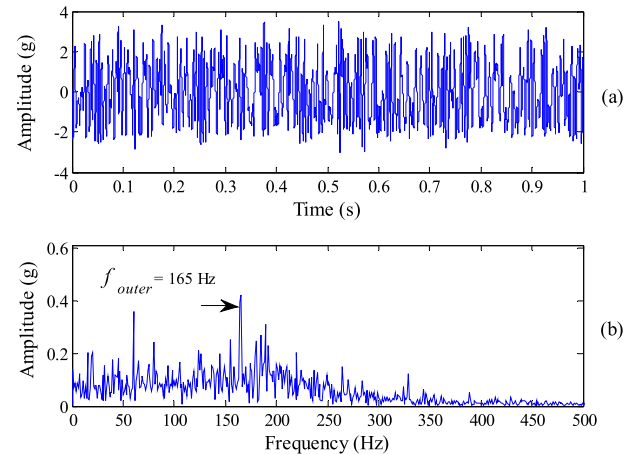

FIGURE 17. Fault characteristic frequency extraction results of the fault bearing vibration signal (outer-ring fault with 1.8mm fault width and 0.6mm fault depth) using the improved UABSR method: (a) Output time domain waveform and (b) its frequency spectrum.

However, the amplitudes of the fault characteristic frequency 164 Hz and its harmonics in Fig. 13 are higher than that in Fig. 14 and 15. The results show that the improved UABSR method is more reliable and effective than the SES infogram and original UABSR method.

In addition, the strength of bearing vibration signal changes with the failure modes of different fault degrees. The monitoring results with different failure sizes are shown Fig. 13, Fig. 16 and Fig. 17, respectively. It can be seen that the spindle bearing fault frequency is easier to be extracted with the increase of the outer-ring fault width. For the smaller outer-ring fault width (0.6 mm), the amplitudes of the fault characteristic frequency 164 Hz and its harmonics in Fig. 16 is lower than that in Fig. 13 and 17; however, the proposed method can still identify the spindle bearing fault characteristic. Comparisons proved that the proposed improved UABSR method can extract spindle bearing fault characteristic under different outer-ring defects levels.

B. FAULT DIAGNOSIS OF SPINDLE BEARING WITH A WORN INNER RACE DAMAGE

Another inner race spindle bearing fault vibration data obtained from the run-to-failure test data of the aviation engine spindle bearing [27] was adopted to verify the robustness of the proposed method. The test rig which was equipped with four Rexnord ZA-2115 double row cylindrical bearings is shown in Fig. 18. Detailed parameters of test bearings are shown in Table 2. An accelerometer was installed on each bearing housing. Vibration data was collected every 10 minutes and the sample rate is 20000 samples per second. The whole process of the bearing run-to-failure test lasted 827 hours from October 22, 2003 to November 25, 2003 and 2156 groups of bearing vibration data are obtained. Each group of data contains 20480 data points. At the end of the experiment, inner race defect occurred in bearing 3. Fig. 19 presents the vibration waveform and its envelope
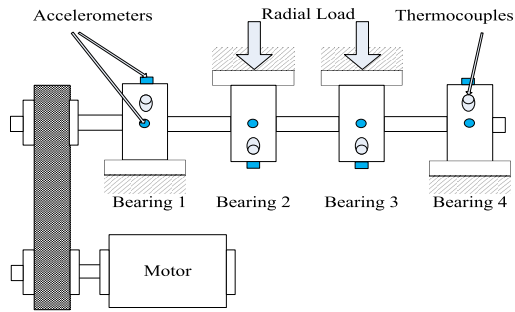
IEEE *Access*

P. Xia *et al.*: Improved Underdamped Asymmetric Bistable SR Method and Its Application for Spindle Bearing Fault Diagnosis

FIGURE 18. Rolling bearing test rig from IMS.

TABLE 2. Geometric parameters of Rexnord ZA-2115.

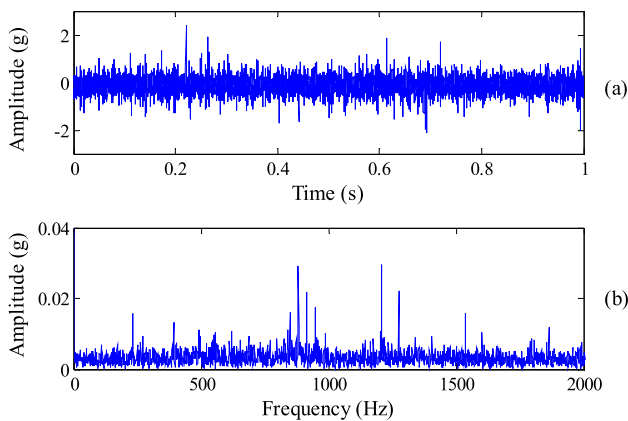| Symbol	Component	Size and value
D_{pitch}	pitch diameter	71.501 mm
D_{roller}	roller diameter	8.407 mm
N	Number of balls	16
f_{inner}	inner ring fault characteristic frequency	296 Hz
α	Initial contact angle	15.17°
ω	inner ring angular velocity	2000 rpm

FIGURE 19. Time domain waveform and envelope frequency spectrum of original vibration signal of spindle bearing with an inner-ring fault: (a) time domain waveform and (b) its frequency spectrum.

frequency spectrum collected from bearing 3 about two hours before the bearing failed and its fault characteristic frequency almost not appear due to the heavy background noise.

The proposed improved UABSR method is used to diagnose the inner ring fault of the aviation engine spindle bearing. After performing the infogram method on the vibration signals of spindle bearing shown in Fig. 19, we choose [2500, 7500] Hz as the suitable frequency band range of the bandpass filter for this working condition. Then, QGAs are used to optimize the parameters pairs (a, b, α, β, m) of the improved UABSR method with the asymmetric bistable potential shown in Eq. (7). According Section 2.4, the adaptive diagnosis result of the improved UABSR method is displayed in Fig. 20 with the parameters
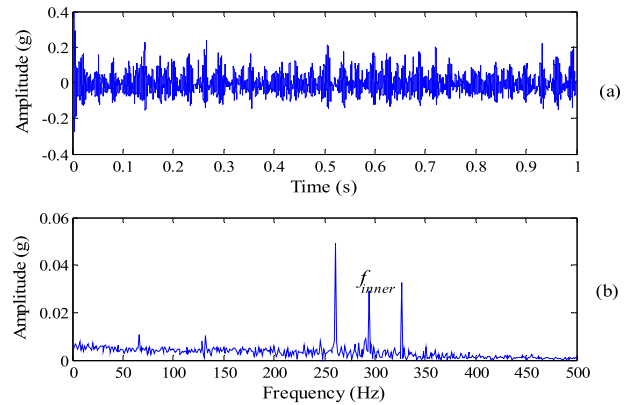

FIGURE 20. Fault characteristic frequency extraction results of the bearing vibration signal with an inner-ring fault using the improved UABSR method: (a) time domain waveform and (b) its frequency spectrum.
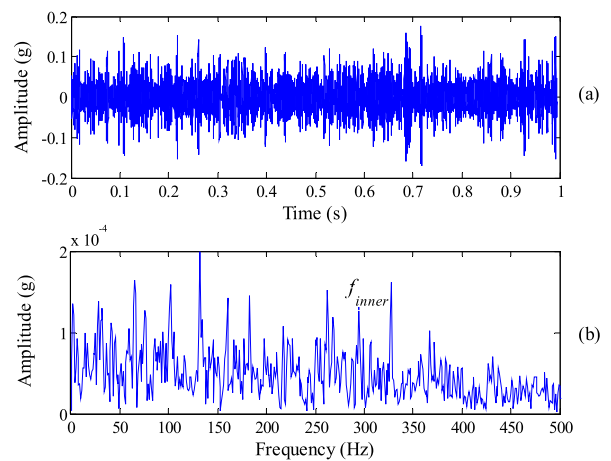

FIGURE 21. Fault characteristic frequency extraction results of the bearing vibration signal with an inner-ring fault using the SES Infogram method: (a) the filtered time domain waveform and (b) its frequency spectrum.
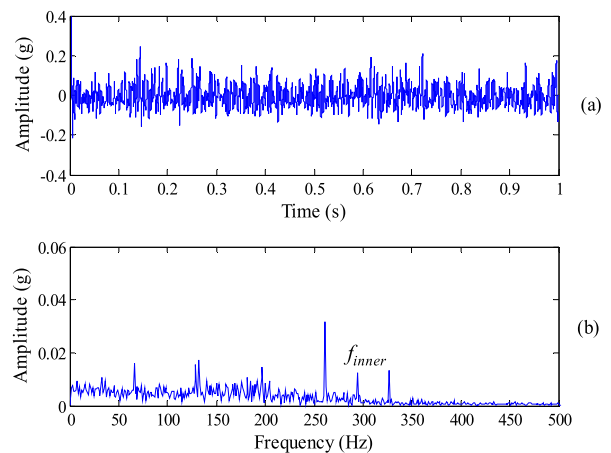

FIGURE 22. Fault characteristic frequency extraction results of the bearing vibration signal with an inner-ring fault using the original UABSR method: (a) time domain waveform and (b) its frequency spectrum.

$(a, b, \alpha, \beta, m) = (2.2147, 2.3948, 4.6685, 0.5492, 875.9672)$. For a fair comparison, the corresponding results of the SES infogram and the original UABSR method (which is

P. Xia *et al.*: Improved Underdamped Asymmetric Bistable SR Method and Its Application for Spindle Bearing Fault Diagnosis

IEEE *Access*

performed by the high-pass filtering) are also displayed in Fig. 21 and 22, respectively. Although the fault characteristic frequency in Fig. 21 and 22 (296 Hz) is extracted from the impact signal with the heavy background noise, there still exists strong interference around the fault characteristic frequency. However, the amplitudes of the fault characteristic frequency 296 Hz and its harmonics in Fig. 20 are higher than that in Fig. 21 and 22. The results also show that the improved UABSR method is more reliable and effective than the SES infogram and original UABSR method.

V. CONCLUSION

An improved UABSR method in an underdamped nonlinear system with a well-width asymmetry bistable potential for incipient spindle bearing fault diagnosis is first proposed. In the proposed improved UABSR method, Infogram method can avoid the influence of impulsive noise and obtain the frequency range of spindle bearing fault. In addition, the TDZC index of the improved UABSR method can directly reflect spindle bearing fault characteristics without knowing the exact fault characteristic frequency in advance. Besides, the optimal system parameter, the asymmetric ratio, the damping factor and the rescaling factor of the improved UABSR model can be obtained simultaneously by using the QGAs and the fourth-order Runge-Kutta algorithm. Comparing the Infogram and original UABSR methods, the simulation and experimental results reveal that the proposed improved UABSR achieves good results in fault diagnosis of spindle bearing faults which are corrupted by heavy background noise.

REFERENCES

[1] H. Xi, H. Y. Wang, W. Han, Y. Le, H. Xu, W. Chen, S. N. Xu, and F. C. Wang, "Contact trajectory of angular contact ball bearings under dynamic operating condition," *Tribol. Int.*, vol. 104, pp. 247–262, Dec. 2016.

[2] C. de Castelbajac, M. Ritou, S. Laporte, and B. Furet, "Monitoring of distributed defects on HSM spindle bearings," *Appl. Acoust.*, vol. 77, pp. 159–168, Mar. 2014.

[3] S. Singh, C. Q. Howard, and C. H. Hansen, "An extensive review of vibration modelling of rolling element bearings with localised and extended defects," *J. Sound Vib.*, vol. 357, pp. 300–330, Nov. 2015.

[4] S. Lu, P. Zhou, X. Wang, Y. Liu, F. Liu, and J. Zhao, "Condition monitoring and fault diagnosis of motor bearings using undersampled vibration signals from a wireless sensor network," *J. Sound Vib.*, vol. 414, pp. 81–96, Feb. 2018.

[5] L. Cui, Y. Zhang, F. Zhang, J. Zhang, and S. Lee, "Vibration response mechanism of faulty outer race rolling element bearings for quantitative analysis," *J. Sound Vib.*, vol. 364, pp. 67–76, Mar. 2016.

[6] J. Li, X. Chen, and Z. He, "Multi-stable stochastic resonance and its application research on mechanical fault diagnosis," *J. Sound Vib.*, vol. 332, no. 22, pp. 5999–6015, Oct. 2013.

[7] Z. Li, X. Liu, T. He, and Y. Shan, "A periodic potential underdamped stochastic resonance method and its application for gear fault diagnosis," *IEEE Access*, vol. 7, pp. 141633–141647, Sep. 2019.

[8] G. W. Vogl and M. A. Donmez, "A defect-driven diagnostic method for machine tool spindles," *CIRP Ann.*, vol. 64, no. 1, pp. 377–380, 2015.

[9] L. Barbini, M. O. T. Cole, A. J. Hillis, and J. L. du Bois, "Weak signal detection based on two dimensional stochastic resonance," in *Proc. 23rd Eur. Signal Process. Conf. (EUSIPCO)*, Piscataway, NJ, USA, Aug./Sep. 2015, pp. 2147–2151.

[10] A. P. Pmpusunggu, S. Devos, and F. Petre, "Stochastic-resonance based fault diagnosis for rolling element bearings subjected to low rotational speed," *Int. J. Prognostics Health Manag.*, vol. 4, pp. 1–15, 2013.

[11] C. He, H. Li, Z. Li, and X. Zhao, "An improved bistable stochastic resonance and its application on weak fault characteristic identification of centrifugal compressor blades," *J. Sound Vib.*, vol. 442, pp. 677–697, Mar. 2019.

[12] C. U. Mba, V. Makis, S. Marchesiello, A. Fasana, and L. Garibaldi, "Condition monitoring and state classification of gearboxes using stochastic resonance and hidden Markov models," *Measurement*, vol. 126, pp. 76–95, Oct. 2018.

[13] K. Shin, "An alternative approach to measure similarity between two deterministic transient signals," *J. Sound Vib.*, vol. 371, pp. 434–445, Jun. 2016.

[14] N. Gunes, M. S. Leeson, and M. D. Higgins, "The use of symmetric quartic potential well for noise filtering," *Fluctuation Noise Lett.*, vol. 17, no. 03, Sep. 2018, Art. no. 1850019.

[15] S. Lu, Q. He, T. Yuan, and F. Kong, "Online fault diagnosis of motor bearing via Stochastic-Resonance-Based adaptive filter in an embedded system," *IEEE Trans. Syst., Man, Cybern. Syst.*, vol. 47, no. 7, pp. 1111–1122, Jul. 2017.

[16] H. Dong, H. Wang, X. Shen, and Z. Jiang, "Effects of second-order matched stochastic resonance for weak signal detection," *IEEE Access*, vol. 6, pp. 46505–46515, Aug. 2018.

[17] Z. Qiao, Y. Lei, J. Lin, and F. Jia, "An adaptive unsaturated bistable stochastic resonance method and its application in mechanical fault diagnosis," *Mech. Syst. Signal Process.*, vol. 84, pp. 731–746, Feb. 2017.

[18] P. Xia, H. Xu, M. Lei, and Z. Ma, "An improved stochastic resonance method with arbitrary stable-state matching in underdamped nonlinear systems with a periodic potential for incipient bearing fault diagnosis," *Meas. Sci. Technol.*, vol. 29, no. 8, Jun. 2018, Art. no. 085002.

[19] Z. Qiao, Y. Lei, J. Lin, and S. Niu, "Stochastic resonance subject to multiplicative and additive noise: The influence of potential asymmetries," *Phys. Rev. E, Stat. Phys. Plasmas Fluids Relat. Interdiscip. Top.*, vol. 94, no. 5, Nov. 2016, Art. no. 052214.

[20] J. Liu, J. Cao, Y. Wang, and B. Hu, "Asymmetric stochastic resonance in a bistable system driven by non-Gaussian colored noise," *Phys. A, Stat. Mech. Appl.*, vol. 517, pp. 321–336, Mar. 2019.

[21] J. Antoni, "The infogram: Entropic evidence of the signature of repetitive transients," *Mech. Syst. Signal Process.*, vol. 74, pp. 73–94, Jun. 2016.

[22] X. Xu, Z. Qiao, and Y. Lei, "Repetitive transient extraction for machinery fault diagnosis using multiscale fractional order entropy infogram," *Mech. Syst. Signal Process.*, vol. 103, pp. 312–326, Mar. 2018.

[23] J. Wang, Q. He, and F. Kong, "Adaptive multiscale noise tuning stochastic resonance for health diagnosis of rolling element bearings," *IEEE Trans. Instrum. Meas.*, vol. 64, no. 2, pp. 564–577, Feb. 2015.

[24] B. Dybiec and E. Gudowska-Nowak, "Stochastic resonance: The role of alpha-stable noises," *Acta Phys. Polonica B*, vol. 37, no. 5, pp. 1479–1490, May 2006.

[25] D. Huang, J. Yang, D. Zhou, and G. Litak, "Novel adaptive search method for bearing fault frequency using stochastic resonance quantified by amplitude-domain index," *IEEE Trans. Instrum. Meas.*, vol. 69, no. 1, pp. 109–121, Jan. 2020.

[26] J. H. Wan, B. He, D. R. Wang, T. H. Yan, Y. Shen, "Fractional-order PID motion control for AUV using cloud-model-based quantum genetic algorithm," IEEE Access, vol. 7, pp. 124828–124843, Sep. 2019.

[27] H. Qiu, J. Lee, J. Lin, and G. Yu, "Wavelet filter-based weak signature detection method and its application on rolling element bearing prognostics," *J. Sound Vib.*, vol. 289, nos. 4–5, pp. 1066–1090, Feb. 2006.
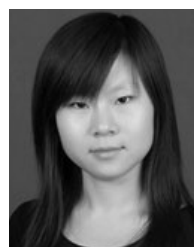
PING XIA received the B.S. degree in mechanical engineering from Jilin Agricultural University, Changchun, China, in 2010, and the M.S. degree in mechanical engineering from the Lanzhou University of Technology, Lanzhou, China, in 2013. She has published three related academic articles in relevant journals indexed by SCI and EI. Her current research interests include dynamic analysis, weak signal characteristic enhancement, and fault diagnosis of precision spindle bearing.

IEEE *Access*

P. Xia *et al.*: Improved Underdamped Asymmetric Bistable SR Method and Its Application for Spindle Bearing Fault Diagnosis

HUA XU was born in Shenyang, China, in 1956. He received the B.S., M.S., and Ph.D. degrees in mechanical engineering from Xi'an Jiaotong University, Xi'an, China, in 2004. He is currently a Professor with Xi'an Jiaotong University. He has participated in more than ten national scientific research projects. He is the author of five books. He has published three related academic articles and more than 80 articles in relevant journals indexed by SCI and EI. His research interests include control, dynamics, and fault diagnosis.

SHENGLUN ZHANG received the B.S. degree in mechanical engineering from Beijing Jiaotong University, Beijing, China, in 2013, and the M.S. degree in mechanical engineering from Xinjiang University, Ürümqi, China, in 2015. He has published three related academic articles in relevant journals indexed by SCI and EI. His current research interests include bearing-rotor system dynamics, active control of rotor vibration, and intelligent bearing.

• • •
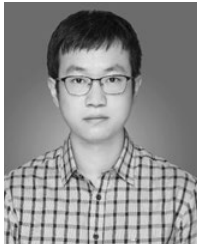
MOHAN LEI received the B.S. degree in mechanical engineering from Tianjin Polytechnical University, Tianjin, China, in 2010, and the M.S. degree in mechanical engineering from the Lanzhou University of Technology, Lanzhou, China, in 2014. He has published four related academic articles in relevant journals indexed by SCI. His current research interests include ultraprecision spindles and bearings, and machine learning applications in industry.